Dynamics of a reaction-diffusion system with Brusselator kinetics under feedback control

Iasson Karafyllis,[1] Panagiotis D. Christofides,[2] and Prodromos Daoutidis[1]
[1]*Department of Chemical Engineering and Materials Science, University of Minnesota, Minneapolis, Minnesota 55455*
[2]*Department of Chemical Engineering, University of California, Los Angeles, California 90095*
(Received 31 December 1997)

This paper studies the dynamics of the reaction-diffusion Brusselator model with Neumann and Dirichlet boundary conditions, under linear and nonlinear modal feedback control. The bifurcation parameters are for the Neumann problem the concentration of one of the reactants and for the Dirichlet problem the diffusion coefficient of one of the reactants. The study of the dynamics of the system is based on methods of bifurcation theory and the application of Poincaré maps. A direct comparison of the dynamics of the open-loop and closed-loop systems establishes that the use of feedback control significantly suppresses the rich open-loop dynamics. In addition, the superiority of the nonlinear controller over a linear controller, in attenuating the effect of bifurcations on the output of the closed-loop system, and the ability of the nonlinear controller to stabilize the system states at the spatially uniform solution provided the number of manipulated inputs is sufficiently large are shown for both the Neumann and Dirichlet problems. [S1063-651X(99)05201-0]

PACS number(s): 05.45.Gg

I. INTRODUCTION

Reaction-diffusion (RD) systems arise frequently in the study of chemical and biological phenomena and are naturally modeled by parabolic partial differential equations (PDEs). The dynamics of RD systems has been the subject of intense research activity over the past decades. The reason is that RD systems exhibit very rich dynamic behavior including periodic and quasiperiodic solutions and chaos (see, for example, [1–4] for some results and reference lists).

A RD system whose dynamics has been studied extensively is the Brusselator reaction scheme in one- and two-dimensional domains. In [5–7] extensive bifurcation studies of the Brusselator model showed that the system exhibits very rich dynamic behavior for different regions in the parameter space. In [8] the dynamics of the Brusselator model with Dirichlet boundary conditions was studied using the length of the domain as the bifurcation parameter and evidence of chaotic behavior was presented. Theoretical justification of the existence of aperiodic solutions based on bifurcation theory was presented in [9], while secondary and homoclinic bifurcations were analyzed in [10–12] for the Brusselator reaction scheme for both one- and two-dimensional domains.

Even though the analysis of complex dynamics of RD systems has been a research subject for more than 30 years, the use of feedback control to supress complex dynamics of RD systems and the study of the dynamics of RD systems under feedback control have been addressed only recently. In [13] a linear adaptive control strategy was applied to the Gray-Scott model in order to control the formation of patterns in a one-dimensional domain, while in [14] an experimental application of linear modal feedback control for suppressing chaotic temporal fluctuations of spatiotemporal thermal patterns on a catalytic wafer was reported. In [8] a feedback controller based on the singular value decomposition of the spatial differential operator was used to control complex dynamics of the Brusselator model and a detailed bifurcation analysis of the closed-loop system was performed. Finally, the effect of linear modal feedback control on the open-loop dynamics of the FitzHugh-Nagumo model was studied in [15].

In this paper we present a study of the dynamics of the RD Brusselator model with Neumann and Dirichlet boundary conditions, under nonlinear and linear modal feedback control. The bifurcation parameters are for the Neumann problem the concentration of one of the reactants and for the Dirichlet problem the diffusion coefficient of one of the reactants. The main objective of the study, which is based on methods of bifurcation theory and the application of Poincaré maps, is to determine to what extent the rich dynamic behavior exhibited by the open-loop system is suppressed by the use of feedback control. The paper is structured as follows. Initially, the process model is presented and an analysis of the open-loop system is performed to determine values of the bifurcation parameter for which Hopf bifurcations occur. Then the nonlinear modal feedback controller is synthesized and the closed-loop system is analyzed. Finally, the projections of the Poincaré maps on suitably chosen planes of the open-loop and closed-loop systems, for various values of the bifurcation parameter, as well as the closed-loop output responses and spatial profiles of the process states under nonlinear and linear control, are presented and compared.

II. PROCESS DESCRIPTION AND MODEL

We consider an isothermal membrane reactor, shown in Fig. 1, where the diffusive phenomena are important in one dimension and the following Brusselator reaction scheme takes place:

$$A \rightarrow X,$$

$$B + X \rightarrow Y + D,$$

$$2X + Y \rightarrow 3X,$$

$$X \rightarrow E.$$

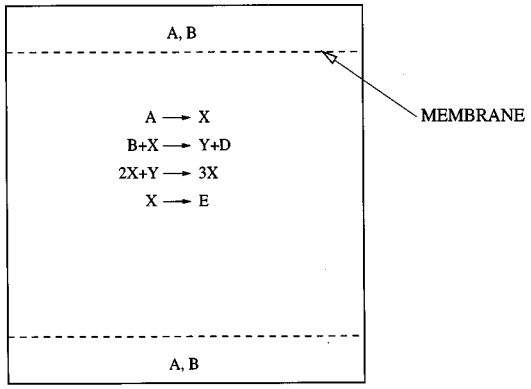

FIG. 1. Isothermal membrane reactor.

In the above reaction scheme, A,B are the reactants and X,Y,D are the products. The concentration of reactant B is assumed to be constant throughout the reactor with value b. Assuming that the concentrations are properly scaled such that the kinetic constants are set equal to 1 and setting $x_1 = X - X_s$ and $x_2 = Y - Y_s$, where $X_s = a$ and $Y_s = b/a$ are the spatially uniform steady states (note that all concentration variables are dimensionless), the dynamics of the process are described by the system of parabolic PDEs

$$\frac{\partial x}{\partial t} = D\Delta x + Ax + f(x) + cu(z,t) \quad \text{in } \Omega \tag{1}$$

subject to the initial condition

$$x(z,0) = x_0(z), \tag{2}$$

where $\Omega = [0,1]$, $x = [x_1 \quad x_2]^T$, x: $\Omega \times [0,+\infty) \to \mathbb{R}^2$, $x_i \in L^2([0,1])$ (the usual Hilbert space of square integrable functions), $i = 1,2$, z denotes the spatial coordinate, t denotes (dimensionless) time, Δ is the one-dimensional Laplacian operator, D and A are constant matrices of the form

$$D = \begin{bmatrix} D_1 & 0 \\ 0 & D_2 \end{bmatrix}, \quad A = \begin{bmatrix} b-1 & a^2 \\ -b & -a^2 \end{bmatrix},$$

$f(x)$ is a nonlinear function of the form

$$f(x) = h(x_1,x_2)\begin{bmatrix} 1 \\ -1 \end{bmatrix}, \qquad h(x_1,x_2) = \frac{b}{a}x_1^2 + 2ax_1x_2 + x_1^2x_2. \tag{3}$$

$c = [1 \quad 0]^T$, and $u(z,t)$ is the deviation of the concentration of species A from the reference value a, which will be considered later as the manipulated variable for the control problem.

We will consider the system of equations (1) with two different sets of boundary conditions: (i) the Neumann (no flux) boundary conditions

$$\frac{\partial x}{\partial z}(0,t) = \frac{\partial x}{\partial z}(1,t) = 0 \tag{4}$$

and (ii) the Dirichlet boundary conditions

$$x(0,t) = x(1,t) = 0. \tag{5}$$

The system of equations (1) clearly admits the uniform in space steady state solution (0,0) for both sets of boundary conditions.

III. DYNAMICAL ANALYSIS OF THE OPEN-LOOP SYSTEM

In this section we consider b to be the bifurcation parameter for the Neumann problem and D_2 to be the bifurcation parameter for the Dirichlet problem and perform spectral analyses of the linearization of the system of equations (1), for both the Neumann and the Dirichlet problem, in order to analytically derive the values of b, D_2 for which Hopf bifurcations occur in the open-loop system, i.e., Eq. (1) with $u(z,t) = 0$ (see also [5,6,9] for similar analyses). We concentrate on Hopf bifurcations because our intention is to study a part of the parametric space where only Hopf bifurcations are possible.

For the Neumann problem a straightforward computation of the eigenvalues and eigenfunctions of the Laplacian operator Δ, subject to the boundary conditions of Eq. (4), yields $\mu_0 = 0$, $\phi_0(z) = 1$, $\mu_n = -n^2\pi^2$, and $\phi_n(z) = \sqrt{2}\cos(n\pi z)$; $n = 1,...,\infty$, where μ_n is an eigenvalue and $\phi_n(z)$ is an eigenfunction. Expanding the solution of the system of equations (1) in an infinite series in terms of the eigenfunctions of the Laplacian operator, we obtain

$$x_i(z,t) = \sum_{n=0}^{\infty} \alpha_{n,i}(t)\phi_n(z), \quad i = 1,2, \tag{6}$$

where $\alpha_{n,i}(t)$ are time-varying coefficients. Substituting the expansion (6) into the system of equations (1) and taking the inner product in $L^2([0,1])$ with the adjoint eigenfunctions of Δ, the following system of infinite ordinary differential equations is obtained:

$$\begin{aligned} \dot{\alpha}_{0,1} &= (b-1)\alpha_{0,1} + a^2\alpha_{0,2} + f_0, \\ \dot{\alpha}_{0,2} &= -b\alpha_{0,1} - a^2\alpha_{0,1} - f_0, \\ \dot{\alpha}_{n,1} &= (-n^2\pi^2 D_1 + b - 1)\alpha_{n,1} + a^2\alpha_{n,2} + f_n, \\ \dot{\alpha}_{n,2} &= -b\alpha_{n,1} - (n^2\pi^2 D_2 + a^2)\alpha_{n,2} - f_n, \end{aligned} \tag{7}$$

where

$$f_n = \int_\Omega \phi_n(z) h\left(\sum_{n=0}^{\infty} \alpha_{n,1}(t)\phi_n(z), \sum_{n=0}^{\infty} \alpha_{n,2}(t)\phi_n(z) \right) dz, \quad n = 0,...,\infty. \tag{8}$$

For the above system, a pair of eigenvalues crosses the imaginary axis when

$$b = b_n = 1 + a^2 + n^2\pi^2(D_1 + D_2), \quad n = 0,...,\infty. \tag{9}$$

Apparently, the smallest value of b where a Hopf bifurcation occurs (see [16] for a justification of this fact for the infinite-dimensional case) is

$$b_0 = 1 + a^2, \tag{10}$$

for which the system of equations (1) admits a periodic uniform in space solution. We note that this periodic solution is also an invariant set for the system of equations (1) with $D_1=D_2=0$.

For the Dirichlet problem the corresponding eigenvalues and eigenfunctions of the Laplacian operator Δ subject to the boundary conditions of Eq. (5) are $\mu_n=-n^2\pi^2$ and $\phi_n(z)=\sqrt{2}\sin(n\pi z)$, $n=1,...,\infty$. Expanding again the solution of the system of equations (1) in an infinite series in terms of the eigenfunctions of the Laplacian operator, we obtain

$$x_i(z,t)=\sum_{n=1}^{\infty}\alpha_{n,i}(t)\phi_n(z),\quad i=1,2, \tag{11}$$

Substituting the expansion (11) into the system of equations (1) and taking the inner product in $L^2([0,1])$ with the adjoint eigenfunctions of Δ, we obtain

$$\begin{aligned}\dot{\alpha}_{n,1}&=(-n^2\pi^2D_1+b-1)\alpha_{n,1}+a^2\alpha_{n,2}+f_n,\\ \dot{\alpha}_{n,2}&=-b\alpha_{n,1}-(n^2\pi^2D_2+a^2)\alpha_{n,2}-f_n,\end{aligned} \tag{12}$$

where $g_n=0$ if n is even and $g_n=2\sqrt{2}/n\pi$ if n is odd and f_n is defined in the same way as Eq. (8). Note that in this case the manipulated variable u appears only in the equations for the odd modes.

For the above system, assuming that $D_1=\lambda D_2=\lambda d$, where λ is a constant positive parameter, a pair of eigenvalues crosses the imaginary axis when

$$d=d_n=\frac{b-1-a^2}{n^2\pi^2(\lambda+1)},\quad n=1,...,\infty. \tag{13}$$

The largest value of d where a Hopf bifurcation occurs for the Dirichlet problem is for $n=1$:

$$d_1=\frac{b-1-a^2}{\pi^2(\lambda+1)}, \tag{14}$$

for which the system of equations (1) admits a periodic solution. Note that this periodic solution is nonuniform in space because the eigenfunction of the mode where the bifurcation occurs is spatially dependent.

IV. FEEDBACK CONTROL: ANALYSIS OF THE CLOSED-LOOP SYSTEM

In this section we assume that measurements of the coefficients $\alpha_{n,i}(t)$ are available and synthesize a nonlinear modal feedback controller for the system of equations (1) by using geometric control methods [17] (see also [18] for an alternative approach for the design of nonlinear feedback controllers for parabolic PDE systems). The assumption that the $\alpha_{n,i}(t)$ are known allows studying the dynamics of the closed-loop system under a feedback controller that does not introduce additional dynamics in the closed-loop system. This is important because it allows a fair comparison between the dynamics of the open-loop and closed-loop systems as well as a precise evaluation of the ability of feedback control to suppress the complex open-loop dynamics. In practice, whenever measurements of $\alpha_{n,i}(t)$ are not available, output feedback controllers, which utilize state observers to estimate the values of $\alpha_{n,i}(t)$ from measurements of the process output, could be employed to regulate the process. The reader may refer to [19] for a methodology for output feedback controller synthesis for quasilinear parabolic PDE systems using the concept of approximate inertial manifold.

A. Output regulation

We consider as controlled output the mean value of the concentration of the component X:

$$y(t)=\int_{\Omega}x_1(z,t)dz \tag{15}$$

or in terms of the modal coefficients

$$y(t)=\alpha_{0,1}(t) \tag{16}$$

for the Neumann problem and

$$y(t)=\sum_{n\ \mathrm{odd}}^{\infty}g_n\alpha_{n,1}(t) \tag{17}$$

for the Dirichlet problem. The control objective is to ensure that the output satisfies $\max_{t\to\infty}|y(t)|\leqslant\epsilon$, where ϵ is a small positive number that depends on the desired closed-loop performance specifications, by using one manipulated input that is distributed uniformly in space, i.e., $u(z,t)=u(t)$.

Applying nonlinear geometric control methods to the systems of equations (7) and (12), one can derive the following feedback laws: (i) For the Neumann problem

$$u=-(b-1+K)y-a^2\alpha_{0,2}-f_0 \tag{18}$$

and (ii) for the Dirichlet problem

$$\begin{aligned}u=&-(b-1+K)y+r\sum_{n\ \mathrm{odd}}^{\infty}n\alpha_{n,1}(t)-a^2\\ &\times\sum_{n\ \mathrm{odd}}^{\infty}g_n\alpha_{n,2}(t)-\sum_{n\ \mathrm{odd}}^{\infty}g_nf_n(t),\end{aligned} \tag{19}$$

which induce the following output response in the corresponding closed-loop systems:

$$\dot{y}=-Ky, \tag{20}$$

where $K>0$ is an adjustable parameter. The application of the controller of Eq. (18) [Eq. (19)] to the system of equations (7) [(12)] would directly lead to the satisfaction of the control objective $\max_{t\to\infty}|y(t)|\leqslant\epsilon$ in the closed-loop system for both problems, for any values of $\epsilon\geqslant 0$, b, and d. However, the implementation of these controllers would require the computation of infinite sums, which cannot be done in practice. Therefore, we approximate the above controllers with the following ones that involve finite sums: (i) For the Neumann problem

$$u=-(b-1+K)y-a^2\alpha_{0,2}-\hat{f}_0 \tag{21}$$

and (ii) for the Dirichlet problem

$$u=-(b-1+K)y+r\sum_{n\ \mathrm{odd}}^{N} n\alpha_{n,1}(t)-a^2\sum_{n\ \mathrm{odd}}^{N} g_n\alpha_{n,2}(t)-\sum_{n\ \mathrm{odd}}^{N} g_n\hat{f}_n(t), \tag{22}$$

where

$$\hat{f}_n=\int_\Omega \phi_n(z)h\left(\sum_{n=n_{\min}}^{N}\alpha_{n,1}(t)\phi_n(z),\sum_{n=n_{\min}}^{N}\alpha_{n,2}(t)\phi_n(z)\right)dz,\quad n=n_{\min},\ldots,N, \tag{23}$$

and $n_{\min}=0$ for the Neumann problem and $n_{\min}=1$ for the Dirichlet problem. The value of N will be determined to ensure that the control objective $\max_{t\to\infty}|y(t)|\leqslant\epsilon$ is enforced in the closed-loop system.

We proceed with a closed-loop stability analysis for the Neumann problem. Substituting the controller of Eq. (21) into the system of equations (7), the infinite-dimensional closed-loop system takes the form

$$\begin{aligned}
\dot{\alpha}_{0,1}&=-K\alpha_{0,1}+(f_0-\hat{f}_0),\\
\dot{\alpha}_{0,2}&=-b\alpha_{0,1}-a^2\alpha_{0,2}-f_0,\\
\dot{\alpha}_{n,1}&=(-n^2\pi^2D_1+b-1)\alpha_{n,1}+a^2\alpha_{n,2}+f_n,\\
\dot{\alpha}_{n,2}&=-b\alpha_{n,1}-(n^2\pi^2D_2+a^2)\alpha_{n,2}-f_n,\\
n&=1,\ldots,\infty,
\end{aligned} \tag{24}$$

where f_n is defined in Eq. (8). The controller of Eq. (21) stabilizes the first two modes, i.e., the two-dimensional system

$$\begin{aligned}
\dot{\alpha}_{0,1}&=-K\alpha_{0,1}+(f_0-\hat{f}_0),\\
\dot{\alpha}_{0,2}&=-b\alpha_{0,1}-a^2\alpha_{0,2}-f_0,
\end{aligned} \tag{25}$$

for which the eigenvalues are $\lambda_{0,1}=-K$ and $\lambda_{0,2}=-a^2$. We also note that when $b<b_1$, the controller of Eq. (21) exponentially stabilizes the infinite-dimensional closed-loop system of equations (24) at the steady state (0,0) and the output approaches 0 asymptotically. However, this stabilizing action does not preclude the presence of bifurcations in the infinite-dimensional closed-loop system of equations (24) for $b>b_1$. In particular, when $b>b_1$ the spatially uniform steady state solution (0,0) is not stable because the remaining uncontrolled modes exhibit oscillatory behavior. Furthermore, in this case $\max_{t\to\infty} y(t)\neq 0$ because of the inexact cancellation of the nonlinear terms in the system of equations (24).

A similar analysis can be also performed for the Dirichlet problem, with the modification that the control law of Eq. (22) leaves the even modes of the infinite-dimensional system of equations (12) completely unaffected. This again means that if $d<d_2$, then the (0,0) steady state becomes unstable and the positively invariant set consists of more complicated orbits in the infinite-dimensional state space. Again, when $d<d_2$ the $\max_{t\to\infty} y(t)\neq 0$ because of the inexact cancellation of the nonlinear terms in the closed-loop system.

B. Spatial profile stabilization

We now consider the problem of stabilizing the entire concentration profile in the case where $b>b_1$ and $d<d_2$ for the Neumann and Dirichlet problems, respectively. This would naturally entail stabilizing every unstable mode of the open-loop system by using more than one manipulated input. To this end, let us define the outputs

$$y_i=\alpha_{i,1},\quad i=n_{\min},\ldots,M, \tag{26}$$

where M denotes the higher integer such that $\alpha_{i,1}$ is unstable, and consider $M+1-n_{\min}$ manipulated inputs [it can be shown by applying standard controllability theory to the linearization of the system of equations (1) that the use of $M+1-n_{\min}$ manipulated inputs suffices to stabilize the entire spatial profile]. We will assume that the ith manipulated input acts uniformly in the spatial interval $[z_i,z_{i+1}]$ and is zero elsewhere, which implies that

$$u(z,t)=\sum_{i=1}^{M+1-n_{\min}} u_i(t)[H(z-z_i)-H(z-z_{i+1})], \tag{27}$$

where $H(z)$ denotes the standard Heaviside function, $z_1=0$, $z_{M+1+n_{\min}}=1$, and $z_{i+1}>z_i$.

Following the same approach as in the output regulation problem, we address the controller design problem on the basis of ordinary differential equations (ODEs) that describe the dynamics of the unstable modes of the PDE system. Specifically, the equations for the unstable modes of the Neumann problem (the development for the Dirichlet problem is similar and will be omitted for brevity) are

$$\begin{aligned}
\dot{\alpha}_{0,1}&=(b-1)\alpha_{0,1}+a^2\alpha_{0,2}+f_0+\sum_{i=1}^{M+1}(z_{i+1}-z_i)u_i,\\
\dot{\alpha}_{n,1}&=(-n^2\pi^2D_1+b-1)\alpha_{n,1}+a^2\alpha_{n,2}+f_n\\
&\quad+\frac{\sqrt{2}}{n\pi}\sum_{i=1}^{M+1}[\sin(n\pi z_{i+1})-\sin(n\pi z_i)]u_i,\\
n&=1,\ldots,M.
\end{aligned} \tag{28}$$

The selection of z_i, $1<i<M+1$, is made so that the linearization of the above system is controllable. The control law is synthesized, using geometric control methods [17], to exponentially stabilize the system of equations (28) and induce a decoupled closed-loop response (the explicit formulas for u_i are omitted for brevity), followed by the truncation of the infinite sums (note that we must have $N>M$) to end up with

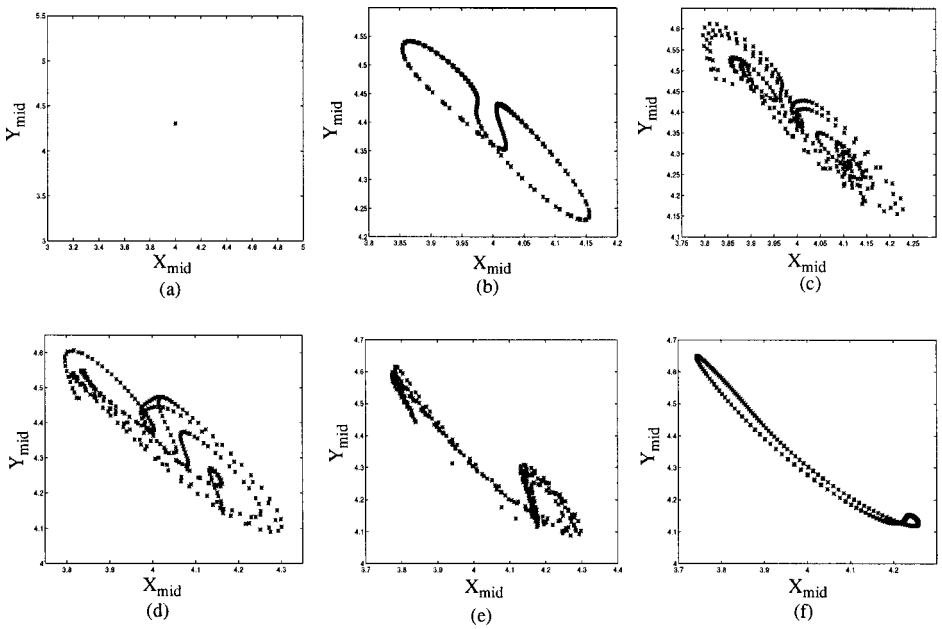

FIG. 2. Poincaré maps of the Neumann problem for (a) $b=17.01$, (b) $b=17.075$, (c) $b=17.095$, (d) $b=17.11$, (e) $b=17.14$, and (f) $b=17.17$.

practically implementable controllers. This results in the equations for the output responses in the closed-loop system

$$\dot{\alpha}_{n,1}=-K\alpha_{n,1}+e_n, \quad n=0,...,M, \tag{29}$$

where e_n is the error due to the truncation of the nonlinear terms. For $K>0$, the steady state $\alpha_{n,1}=0$, $n=0,...,M$, of the closed-loop ODE system is locally (i.e., for sufficiently small initial conditions) exponentially stable. Furthermore, since all the unstable modes of the process have been included in the system of equations (28) and the nonlinear controllers do not employ linear feedback of modes higher than $M+1$, the open-loop stability of modes higher than $M+1$ (i.e., $\alpha_{M+\kappa,1}$, $\kappa=1,...,\infty$) is preserved in the closed-loop system. Finally, the modes $\alpha_{n,2}$ exponentially stabilize as the outputs are exponentially stabilized. The above analysis implies that the steady state (0,0) of the closed-loop infinite-dimensional system is also locally exponentially stable.

V. NUMERICAL RESULTS

In this section we study the dynamics of the open-loop and closed-loop systems for various values of the bifurcation parameter. The numerical values of the process and controller parameters were selected to be (i) $a=4$, $D_1=0.01$, $D_2=0.001$, $K=80$, $\epsilon=0.12$, and $N=4$ for the Neumann problem and (ii) $a=2$, $\lambda=2$, $b=5.45$, $K=80$, $\epsilon=0.002$, and $N=4$ for the Dirichlet problem. For these values $b_0=17.0$, $b_1=17.108$ and $d_1=0.0152$, $d_2=0.0038$, respectively, for the two problems. For the numerical simulation of the system, we used finite differences for the spatial discretization (50 equispaced discretization points were chosen) and a variable step size Runge-Kutta method for time integration.

Poincaré maps are used as a means to present the dynamic behavior of the open-loop and closed-loop systems in a compact fashion. We selected to present the projection of the Poincaré map defined as $x_1(0.3,t)=0$ and $(dx_1/dt)(0.3,t)>0$, on the plane $(X_{\mathrm{mid}},Y_{\mathrm{mid}})=(x_1(0.5,t)+a,x_2(0.5,t)+b/a)$. We are going to use the term ''Poincaré map'' for the previously defined projection of the actual Poincaré map in order to be compatible with the literature [8,3]. It is also reminded that a single point on the Poincaré map indicates periodic behavior, while a closed orbit indicates quasiperiodic behavior.

For the open-loop system the gradual change of the dynamics of the Neumann problem, as b increases from the value of the first Hopf bifurcation $b_0=17.0$, is shown in Fig. 2. The system evolves from a periodic solution (a) to solutions with very complicated dynamics (b)–(f). These solutions seem to be globally stable, i.e., for a given value of b, the system trajectory starting from arbitrary initial conditions ultimately approaches the attractor. We also verified through simulations that for values of b that are very close to b_0 (as the theory predicts), the oscillations of the concentrations are

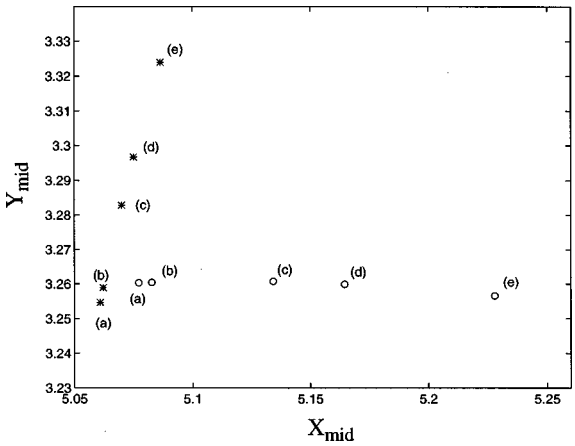

FIG. 3. Poincaré maps for the closed-loop system of the Neumann problem under nonlinear (*) and linear (○) controllers for (a) $b=17.14$, (b) $b=17.17$, (c) $b=17.34$, (d) $b=17.44$, and (e) $b=17.64$.

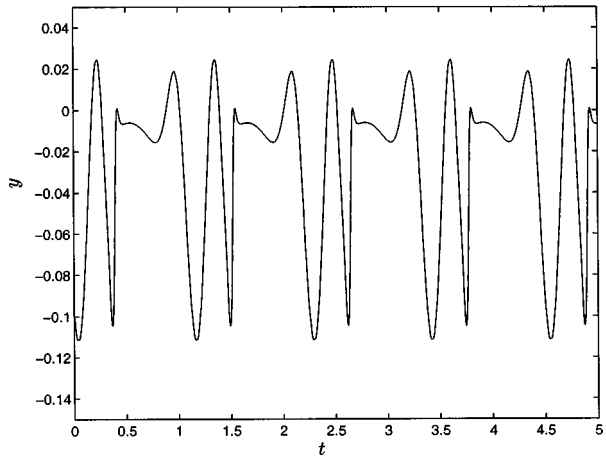

FIG. 4. Closed-loop response of the output y of the Neumann problem under a nonlinear controller with $b=17.14$.

uniform in space, while for higher values of b, symmetry-breaking bifurcations occur that give rise to spatially nonuniform oscillations.

Figure 3 shows the Poincaré maps for the closed-loop system of the Neumann problem under the nonlinear modal feedback controller of Eq. (21) for various values of the bifurcation parameter b. For each value of b the Poincaré map consists of one point, indicating a periodic solution for the closed-loop system. We note that this periodic behavior is spatially nonuniform because it occurs for $n \geqslant 1$, where the eigenfunctions of these modes are spatially dependent. It is clear that the nonlinear controller suppresses the rich dynamic behavior exhibited by the open-loop system. For the sake of comparison, we also study the dynamics of the closed-loop system under a linear controller obtained by neglecting the nonlinear term $\hat{f}_0$ in the controller of Eq. (21), i.e.,

$$u=-(b-1+K)\alpha_{0,1}-a^2\alpha_{0,2}. \tag{30}$$

The Poincaré maps of the closed-loop system, for different values of the bifurcation parameter b, are shown in Fig. 3; they consist of one point indicating that the complicated open-loop dynamics has been suppressed.

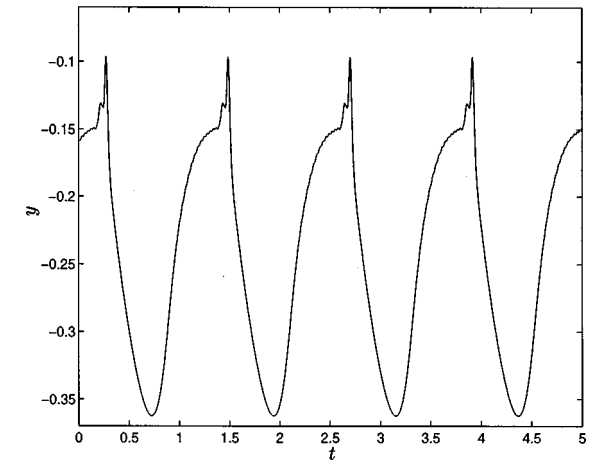

FIG. 5. Closed-loop response of the output y of the Neumann problem under a linear controller with $b=17.14$.

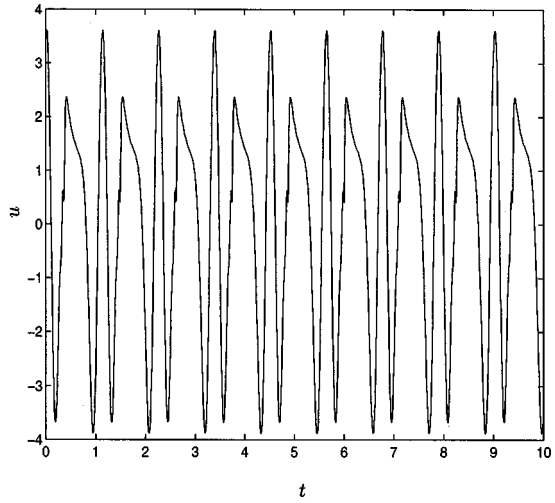

FIG. 6. Evolution of the input for the Neumann problem under a nonlinear controller.

Next we evaluate the ability of modal feedback control to attenuate the effect of bifurcations on the output of the closed-loop system and enforce $\max_{t\to\infty}|y| \leqslant 0.12$. Figure 4 shows the output of the closed-loop system under the nonlinear controller of Eq. (21) for $b=17.14>b_1$. Clearly, the controller attenuates the effect of bifurcations on the closed-loop output (note that the requirement $\max_{t\to\infty}|y| \leqslant 0.12$ is satisfied), but it cannot completely eliminate their effect on the output due to inexact cancellation of the nonlinear terms in the system of equations (24). Figure 5 shows the output of the closed-loop system under the linear controller of Eq. (30) for $b=17.14>b_1$. The output again oscillates, but in this case the amplitude of oscillation is much higher (the requirement $\max_{t\to\infty}|y| \leqslant 0.12$ is *not* satisfied; compare also Figs. 4 and 5; note the scale). The inputs of the nonlinear and linear controller are shown in Figs. 6 and 7 respectively.

For the Dirichlet problem the situation is different. In Fig. 8 we show the Poincaré maps for the open-loop system and for a gradual decrease of the value of d. Although for values

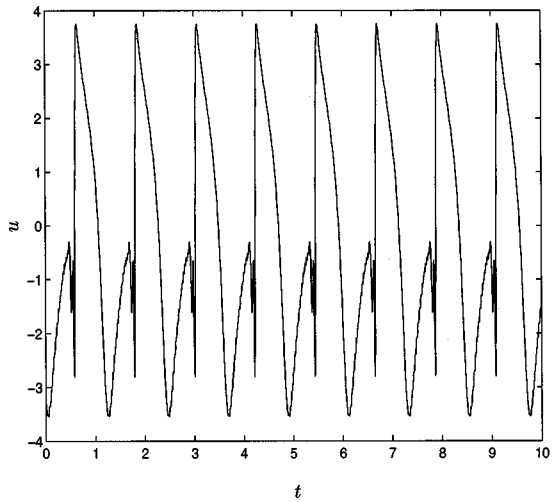

FIG. 7. Evolution of the input for the Neumann problem under a linear controller.

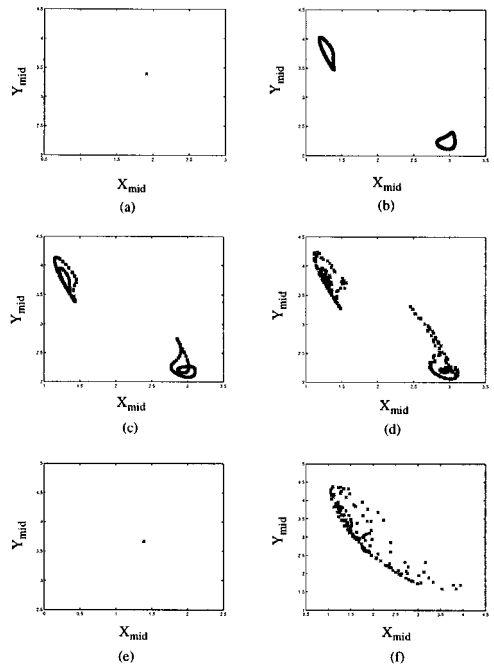

FIG. 8. Poincaré maps of the Dirichlet problem for (a) $d=0.01$, (b) $d=0.002\,03$, (c) $d=0.002\,01$, (d) $d=0.001\,98$, (e) $d=0.0015$, and (f) $d=0.0008$.

of d close to d_1 there is only one attractor (the periodic solution), for smaller values of d ($d<d_2$) there are two attractors (which are obtained for different sets of initial conditions and are reported also in [8]) that consist of quasiperiodic and chaotic solutions. However, for even smaller values of d the attractors seem to coincide or one of them seems to become unstable. It is worth noting that for d close to d_3 the attractor consists again of a periodic solution, but for d close to d_4 the attractor becomes again very complicated. For the closed-loop system under the nonlinear control of Eq. (22) the corresponding Poincaré maps are shown in Fig. 9. It is clear again that the feedback law suppressed the rich dynamics of the open-loop system. Note also that the periodic solution represented in the Poincaré map by one point is obtained for all sets of initial conditions, indicating that the feedback law has made this periodic solution a global attractor.

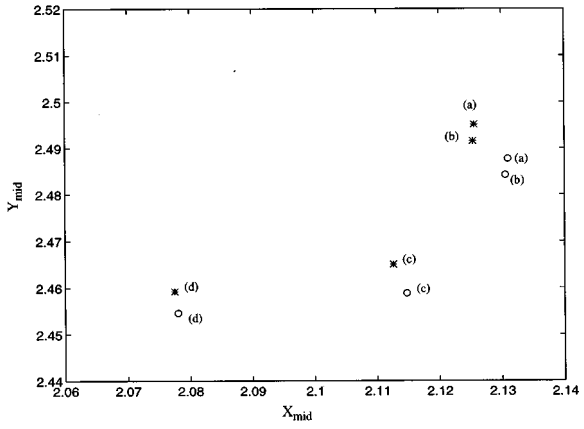

FIG. 9. Poincaré maps for the closed-loop system of the Dirichlet problem under nonlinear (*) and linear (○) controllers for (a) $d=0.002\,03$, (b) $d=0.001\,983\,7$, (c) $d=0.0015$, and (d) $d=0.0008$.

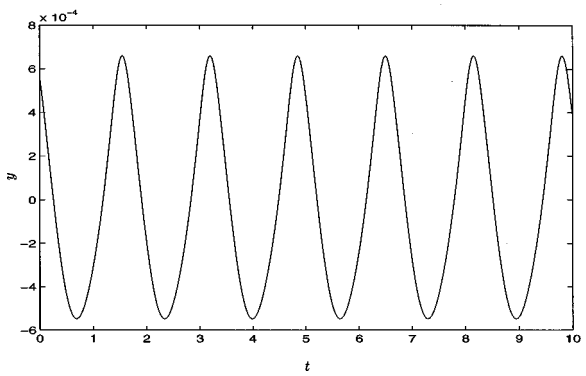

FIG. 10. Closed-loop response of the output y of the Dirichlet problem under a nonlinear controller for $d=0.001\,983\,7$.

In Figs. 10 and 11 we show the output behavior for $d=0.001\,983\,7$ under the nonlinear control law of Eq. (22) with $N=4$ and the linear control law that is obtained by neglecting the nonlinear terms in Eq. (22):

$$u=-(b-1+K)y+r\sum_{n\ \mathrm{odd}}^{N} n\alpha_{n,1}(t)-a^2\sum_{n\ \mathrm{odd}}^{N} g_n\alpha_{n,2}(t). \tag{31}$$

It is clear again that the output oscillates, but in the case of the nonlinear control law the amplitude of the oscillation is much lower than in the case of the linear control law. Note again that the output behavior under the linear control does not satisfy the requirement $\max_{t\to\infty}|y|\leqslant 0.002$. The inputs of the nonlinear and linear controller are shown in Figs. 12 and 13, respectively.

Finally, for the profile stabilization case, we will consider the case of two unstable modes for both the Dirichlet and the Neumann problem, obtained for the following values of the bifurcation parameters: (i) $b_1<b=17.14<b_2$ for the Neumann problem and (ii) $d_3<d=0.003<d_2$ for the Dirichlet problem. We considered two manipulated inputs acting uniformly in the intervals $[0,\frac{1}{2}]$ and $[\frac{1}{2},1]$, respectively, i.e.,

$$u(z,t)=u_1(t)[H(z)-H(z-\tfrac{1}{2})]+u_2(t)[H(z-\tfrac{1}{2})-H(z-1)]. \tag{32}$$

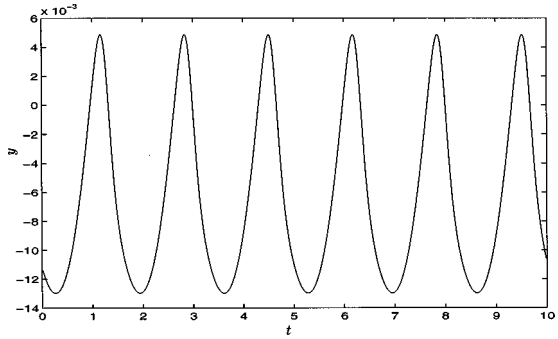

FIG. 11. Closed-loop response of the output y of the Dirichlet problem under a linear controller for $d=0.001\,983\,7$.

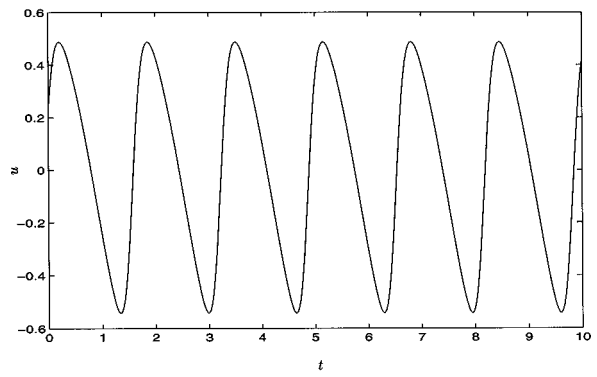

FIG. 12. Evolution of the input for the Dirichlet problem under a nonlinear controller.

The following control laws were implemented: (i) For the Neumann problem

$$u_1 = -(K+b-1)\alpha_{0,1} - a^2\alpha_{0,2} - \hat{f}_0 - \frac{\pi}{2\sqrt{2}}(K+b-1-\pi^2 D_1)\alpha_{1,1} - \frac{\pi a^2}{2\sqrt{2}}\alpha_{1,2} - \frac{\pi}{2\sqrt{2}}\hat{f}_1, \quad (33)$$

$$u_2 = -(K+b-1)\alpha_{0,1} - a^2\alpha_{0,2} - \hat{f}_0 + \frac{\pi}{2\sqrt{2}}(K+b-1-\pi^2 D_1)\alpha_{1,1} + \frac{\pi a^2}{2\sqrt{2}}\alpha_{1,2} + \frac{\pi}{2\sqrt{2}}\hat{f}_1 \quad (34)$$

and (ii) for the Dirichlet problem:

$$u_1 = -\frac{\pi}{2\sqrt{2}}(\hat{f}_1+\hat{f}_2) - \frac{\pi}{2\sqrt{2}}[(b-1-\pi^2 D_1+K)\alpha_{1,1} + a^2(\alpha_{1,2}+\alpha_{2,2}) + (b-1-4\pi^2 D_1+K)\alpha_{2,1}], \quad (35)$$

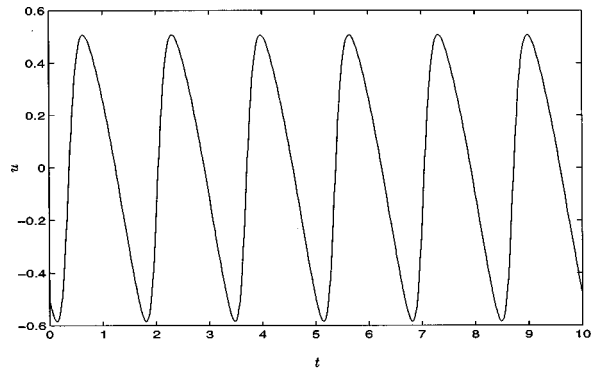

FIG. 13. Evolution of the input for the Dirichlet problem under a linear controller.

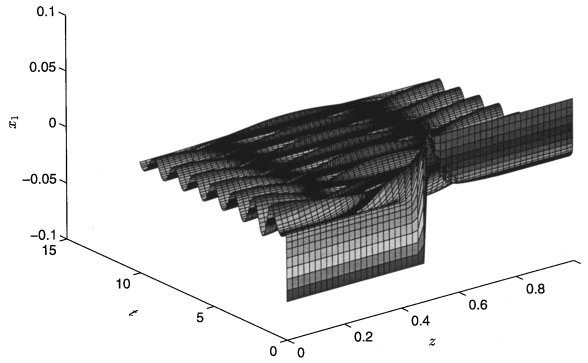

FIG. 14. Profile evolution of the Neumann problem under a nonlinear controller for $b = 17.14$.

$$u_2 = -\frac{\pi}{2\sqrt{2}}(\hat{f}_1-\hat{f}_2) - \frac{\pi}{2\sqrt{2}}[(b-1-\pi^2 D_1+K)\alpha_{1,1} + a^2(\alpha_{1,2}-\alpha_{2,2}) - (b-1-4\pi^2 D_1+K)\alpha_{2,1}], \quad (36)$$

in order to induce the closed-loop response of Eq. (29) and hence stabilize the spatial profile at (0,0). The initial conditions were chosen to be piecewise uniform functions with a very steep gradient at the center of the domain, in order to test the controller performance under conditions of no smoothness in the initial condition. For both cases, it is observed in Figs. 14 and 15 that the controller very quickly moves the spatial profile close to $x_1(z,t) = x_2(z,t) = 0$. Note that the rate of the stabilization depends also on the rate by which the first stable mode exponentially approaches zero. This mode exhibits oscillatory behavior with exponentially decreasing amplitude, which explains the pattern of the oscillation observed in the evolution of the spatial profiles [$\sim\cos(\pi z)\cos(\omega t)$ in the Neumann problem and $\sim\sin(3\pi z)\cos(\omega t)$ in the Dirichlet problem, where ω is the frequency of the oscillation]. The inputs, as it is shown in Figs. 16 and 17, also very quickly approach the value of zero, indicating that the two outputs have also become almost zero in both cases. The above results indicate that even though the distribution functions of the two control actuators are quite sharp [note that $b_1(z) = H(z) - H(z-0.5)$ and $b_2(z) = H(z-0.5) - H(z-1)$] and therefore the control actions affect the modes of the PDE system that were not included in the approximate ODE system used for controller

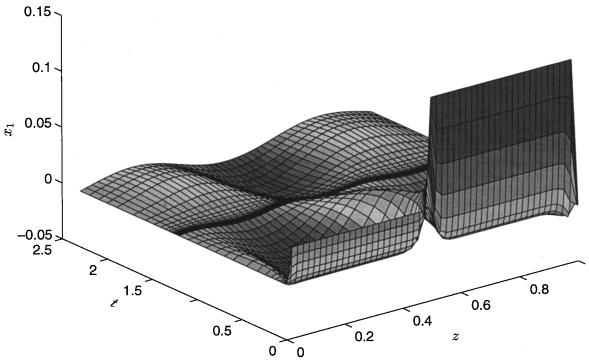

FIG. 15. Profile evolution of the Dirichlet problem under a nonlinear controller for $d = 0.003$.

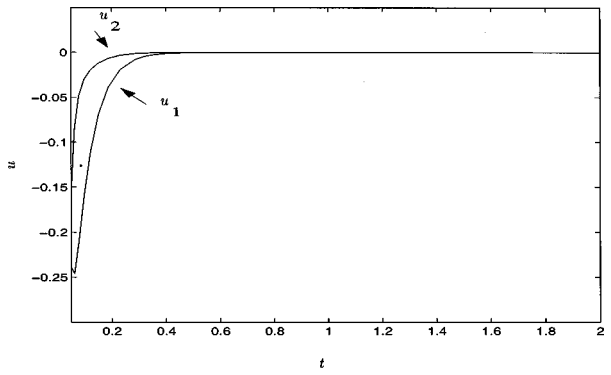

FIG. 16. Evolution of the inputs for the Neumann problem under a nonlinear profile regulating controller for $b = 17.14$.

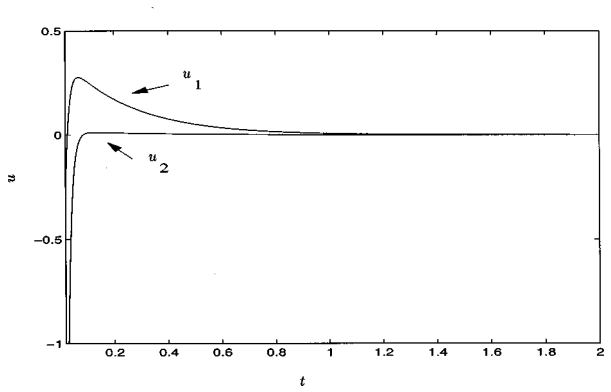

FIG. 17. Evolution of the inputs for the Dirichlet problem under a nonlinear profile regulating controller for $d = 0.003$.

design (spillover effect), these modes are extremely stable and attenuate the effect of spillover.

VI. CONCLUSIONS

In this paper we presented a study of the dynamics of the reaction-diffusion Brusselator model with Neumann and Dirichlet boundary conditions, under modal feedback control. The main conclusions of our study are that (a) the use of modal feedback control drastically suppresses the rich open-loop dynamics, (b) nonlinear control achieves significantly better attenuation of the effect of bifurcations on the closed-loop output than linear control, and (c) the stabilization of the entire spatial profile can be achieved by using a sufficiently large number of manipulated inputs.

ACKNOWLEDGMENT

Financial support for this work by the National Science Foundation under Grant No. CTS-9624725 is gratefully acknowledged.

[1] R. Temam, *Infinite-Dimensional Dynamical Systems in Mechanics and Physics* (Springer-Verlag, Berlin, 1993).
[2] J. Smoller, *Shock Waves and Reaction-Diffusion Equations* (Springer-Verlag, Berlin, 1994).
[3] M. Marek and I. Schreiber, *Chaotic Behavior of Deterministic Dissipative Systems* (Cambridge University Press, New York, 1991).
[4] D. Barkley and I. G. Kevrekidis, Chaos **4**, 453 (1994).
[5] F. G. Auchmuty and F. G. Nicolis, Bull. Math. Biol. **37**, 323 (1975).
[6] F. G. Auchmuty and F. G. Nicolis, Bull. Math. Biol. **38**, 325 (1976).
[7] M. Herschkowitz-Kaufman, Bull. Math. Biol. **37**, 589 (1975).
[8] S. Chakravarti, M. Marek, and W. H. Ray, Phys. Rev. E **52**, 2407 (1995).
[9] J. Guckenheimer, in *Dynamical Systems and Turbulence, Warwick*, Lecture Notes in Mathematics Vol. 898 (Springer-Verlag, Berlin, 1981), pp. 99–142.
[10] M. Herschkowitz-Kaufman and T. Erneux, Ann. (N.Y.) Acad. Sci. **78**, 296 (1979).
[11] J. P. Keener, Stud. Appl. Math. **55**, 187 (1976).
[12] J. P. Keener, SIAM (Soc. Ind. Appl. Math.) J. Appl. Math. **41**, 127 (1981).
[13] V. Petrov, S. Metens, P. Borckmans, G. Dewel, and K. Showalter, Phys. Rev. Lett. **75**, 2895 (1995).
[14] F. Qin, E. E. Wolf, and H.-C. Chang, Phys. Rev. Lett. **72**, 1459 (1994).
[15] S. Y. Shvartsman and I. G. Kevrekidis, AIChE. J. **44**, 1579 (1998).
[16] D. H. Sattinger, *Group Theoretic Methods in Bifurcation Theory*, Lecture Notes in Mathematics Vol. 762 (Springer-Verlag, Berlin, 1979).
[17] A. Isidori, *Nonlinear Control Systems: An Introduction* (Springer-Verlag, Berlin, 1989).
[18] C. C. Chen and H.-C. Chang, AIChE. J. **38**, 1461 (1992).
[19] P. D. Christofides and P. Daoutidis, J. Math. Anal. Appl. **216**, 398 (1997).